Chapter 4
Quantum Simulation of Non-Markovian Qubit Dynamics by an All-Optical Setup

Claudia Benedetti, Simone Cialdi, Matteo A. C. Rossi, Bassano Vacchini, Dario Tamascelli, Stefano Olivares and Matteo G. A. Paris

Abstract We address the experimental implementation of a quantum simulator based on an optical setup. Our device can simulate the dynamical evolution of a qubit undergoing a dephasing process. In particular, we focus on the dynamics arising from the interaction with a classical stochastic field. We encode the state of the qubit in the polarization of a single photon, while the realizations of the stochastic evolution affect its spectral components by a programmable spatial-light-modulator. This setup can simulate in one shot the ensemble-averaged dynamics of the dephasing qubit. We experimentally reconstruct the system density matrix and we show how it is possible to move from a Markovian to a non-Markovian quantum map by changing the spectral parameter of the simulated noise.

4.1 Introduction

Simulating the quantum dynamics of a system may be a challenging task. As pointed out by Feynman [1], the problem may be tackled by considering another quantum controllable system that emulates the systems under study.

General-purpose quantum computers would be formidable and flexible tools able to efficiently reproduce the behavior of a large class of quantum systems. But quantum computers have not been built yet. On the other hand, much attention has been recently devoted to the development of *ad-hoc* quantum simulators [2], i.e. special-

C. Benedetti (✉) · S. Cialdi · M. A. C. Rossi · B. Vacchini · D. Tamascelli
S. Olivares · M. G. A. Paris
Quantum Technology Lab, Dipartimento di Fisica "Aldo Pontremoli",
Università degli Studi di Milano, 20133 Milan, Italy
e-mail: claudia.benedetti@unimi.it
URL: https://users.unimi.it/aqm

S. Cialdi · B. Vacchini
INFN, Sezione di Milano, 20133 Milan, Italy

P. F. Bortignon et al. (eds.), *Toward a Science Campus in Milan*,
https://doi.org/10.1007/978-3-030-01629-6_4

purpose devices that are designed to mimic the dynamics of other specific complex quantum systems that are not easily accessible or controllable, such as large quantum systems, with many degrees of freedom. The inherent parallel structure of quantum simulators make them the perfect candidates to solve problems that are intractable on conventional supercomputers.

In this paper, we explain in detail how it is possible to build a quantum simulator using only optical elements. In particular, we describe how to mimic the dynamical evolution of a single qubit noisy channels originating from the interaction with different fluctuating stochastic fields [3, 4]. The simulated dynamics corresponds to effective models for the interaction of qubits with complex classical environments [5, 6]. We encode the state of a qubit in the polarization degree of freedom of a single photon, while the spectral components play the role of the external environment. The different realizations of the stochastic fluctuations are numerically simulated and imposed to the dynamics via a spatial light modulator.

As a proof of principle, we simulate the dynamics of a qubit undergoing a dephasing dynamics; this is done by performing a sample average over a large number of parallel realizations of the stochastic fluctuations. We moreover provide examples of quantum channels with different degrees of non-Markovianity.

The paper is organized as follows: in Sect. 4.2 we introduce the theoretical model of a dephasing map induced by classical noise; in Sect. 4.3 we explain in detail the implementation and functioning of our quantum simulator. Section 4.4 closes the paper with final remarks.

4.2 The Model

We aim to simulate the dynamics of a qubit interacting with a classical fluctuating field $X(t)$, whose evolution is described by a stochastic process. The time-dependent stochastic Hamiltonian of the system is described by:

$$H(t) = \epsilon\sigma_z + X(t)\sigma_z \tag{4.1}$$

where ϵ is the energy splitting of the qubit and σ_z is the Pauli matrix. Since $X(t)$ is a stochastic process, the evolved qubit state is calculated by performing the ensemble average over all possible realizations of the noise, namely

$$\rho(t) = \left\langle U(t)\rho(0)U^\dagger(t)\right\rangle_{\{X(t)\}} \tag{4.2}$$

for any initial state $\rho(0)$, the unitary operator $U(t) = \exp\left[-i\int H(s)\mathrm{d}s\right]$ represents, instead, the evolution as determined by a particular realization of the process $X(t)$. Without losing generality, we can fix the initial state of the qubit to be the $|+\rangle = \frac{1}{\sqrt{2}}(|0\rangle + |1\rangle)$ state. The generated dynamics in the interaction picture is calculated from (4.2) and its general form is:

$$\rho(t) = \frac{1}{2}\begin{pmatrix} 1 & \langle e^{-2i\varphi(t)}\rangle \\ \langle e^{2i\varphi(t)}\rangle & 1 \end{pmatrix} \tag{4.3}$$

where $\langle e^{-2i\varphi(t)}\rangle$ is the decoherence factor and $\varphi(t) = \int_0^t X(s)\mathrm{d}s$. The decoherence factor can be calculated only once the master equation of the stochastic process $X(t)$ is known. To this aim we consider two stochastic processes, the random telegraph noise (RTN) and the Ornstein-Uhlenbeck (OU) process [7–9]. The generated dynamics is a dephasing map, which preserves the populations in the computational basis and only affects the off-diagonal elements through the decoherence factor.

The RTN is a Markovian Gaussian stochastic process. In this case $X(t) \in \{+1, -1\}$, namely it switches between two values, with a fixed switching rate γ. It is characterized by an exponential autocorrelation function

$$C(t - t_0) = e^{-2\gamma|t-t_0|}. \tag{4.4}$$

If we discretize time and consider a small time interval δt, then the probability for the RTN to flip its value within δt is given by $\delta P = 1 - e^{-\gamma\delta t}$.

On the contrary, the OU process is a Gaussian process, described by the stochastic equation

$$X(t + \delta t) = (1 - 2\gamma\delta t)X(t) + 2\sqrt{\gamma}\mathrm{d}W(t), \tag{4.5}$$

with $\mathrm{d}W(t)$ a Wiener process with zero mean and standard deviation $\sigma = \sqrt{\gamma}$. The OU process has the same autocorrelation function as the RTN, even though the statistics of the two processes are different. For both RTN and OU the decoherence factor is a real quantity, and takes the expressions:

$$\langle e^{-2i\varphi(t)}\rangle_{\mathrm{RTN}} = e^{-\gamma t}\left(\cosh\delta t + \frac{\gamma}{\delta}\sinh\delta t\right) \quad \text{with } \delta = \sqrt{\gamma^2 - 4}, \tag{4.6}$$

$$\langle e^{-2i\varphi(t)}\rangle_{\mathrm{OU}} = e^{-2\beta(t)} \quad \text{with } \beta(t) = \frac{1}{\gamma^2}\left(\gamma t + e^{-\gamma t} - 1\right). \tag{4.7}$$

Given a certain quantum open dynamics, we can ask if memory effects play a role in the characteristics of such map. As classical processes can be classified into Markovian and non-Markovian (NM), various attempts to generalize such memory effects also in quantum dynamics have been made [10–12]. However a unique definition does not exist. One proposal consists in evaluating the non-Markovianity of the dynamical map as the amount of information backflow into the system from the environment [13]. This is calculated by analyzing the revivals of the trace distance $C(t) = \frac{1}{2}\mathrm{Tr}|\rho_1(t) - \rho_2(t)|$ between a pair of initial states of the system. Whenever the trace distance has revivals in time, the dynamics is called non-Markovian, while a monotonic behavior of the trace distance is associated to a Markovian evolution. The difficulty in calculating such NM lies in the optimization over all possible initial pairs of states that is required in order to make the measurement independent of the initial state. In the case of a dephasing dynamics the analytical expression of the maximized trace distance is know and it is equal to the absolute value of the dephasing factor [5, 14]

$$C(t) = \left|\langle e^{-2i\varphi(t)}\rangle\right| . \tag{4.8}$$

When we consider noisy dephasing dynamics arising from the RTN, the NM behavior of the map changes from Markovian for large values of the switching rate, to non-Markovian for small values of γ. On the contrary, OU-generated dynamics are always Markovian. Being able to simulate the evolution of a quantum system and to control its degree of non-Markovianity or the transition between a Markovian to a NM dynamics, is a very important step in the building and implementation of efficient protocols for quantum communications and quantum information technologies [15–17].

4.3 The Physical Implementation

In order to simulate experimentally this dephasing dynamics we use an all-optical setup [3, 4]. In Fig. 4.1 we show a schematic diagram of the experimental apparatus. The frequency-entangled two-photon state is generated by parametric down-conversion (PDC). We use a diode pump laser @ 405.5 nm, that is temperature stabilized and generates 40 mW @ 70 mA, and a BBO crystal 1 mm thick. The two photons are then collected by two fiber couplers and sent respectively into a single-spatial-mode and polarization-preserving fiber (SMF) and a multimode fiber (MMF). When the idler photon enters the coupler, it travels entirely through the fiber towards the single photon detector (D2). Conversely, the signal photon, after a short fiber (SMF), enters a 4F system [18], i.e. propagates in the air, through few optical devices, the gratings G1 and G2 (1714 lines/mm) and lens L1 and L2 ($f = 500$ mm), an half-wave plate (H1), that we use for the input state preparation, a spatial light modulator (SLM) and a tomographic apparatus (T) to reconstruct the output state. The SLM is a 1D liquid crystal mask (640 pixels, 100 μm/pixel) and is placed on the Fourier plane of the 4f system, between the two lenses L1 and L2 (see Fig. 4.1), where the spectral components of the signal photon are linearly dispersed and focalized (1.82 nm/mm, waist = 60 μm). At the end of the 4F system the signal photon is coupled to a multimode fiber and reaches the single photon detector (D1). The two single photon detectors (D1, D2) are based on the avalanche photodiode $C30921S$ in a passive Geiger mode configuration. Finally an electronic device based on the Ortec 567 TAC/SCA measures the coincidence counts (CC) and sends them to the computer (PC) via the National Instruments card PCI6602. The tomographic apparatus (T) [19, 20] is composed of a quarter-wave plate (Q), an half-wave plate (H) and a polarizer (P). The SLM is controlled by the computer (PC) and is used to introduce a different phase $\varphi_r(t)$ for each pixel.

The experimental setup described above implements our quantum simulator by performing the following steps: the quantum information carrier is a single photon generated by the parametric down-conversion and its polarization is used to encode the state of a qubit; its spectral components are instead exploited to simulate a classical fluctuating field. Specifically, the realizations of the stochastic processes are achieved

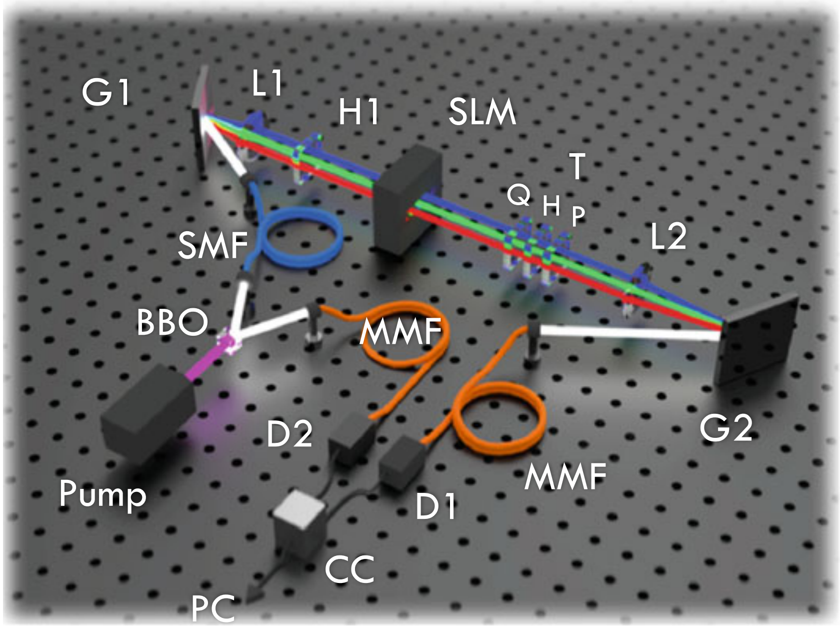

Fig. 4.1 Schematic diagram of our experimental setup. Pump, 405.5 nm laser diode; BBO, Beta barium borate nonlinear crystal; SMF, single-spatial-mode and polarization preserving fiber; MMF, multimode fiber; G1–G2, gratings; L1–L2, lens; H1, half-wave-plate; SLM, spatial light modulator; T, tomographic apparatus; D1–D2, single photon detectors; CC, coincidences counter

in a single shot by using the programmable SLM on the different spectral components of the same photon. The photon is initialized in the state $|\psi_0\rangle = \frac{1}{\sqrt{2}}(|H\rangle + |V\rangle)$ by the H1 plate. By exploiting the quantum nature of the photon, we are able to simulate in one shot the ensemble average over n realizations of the noise. This is accomplished by first numerically simulating on a computer the different n trajectories of the random phases $\varphi(t)$ appearing in (4.3) which are applied only on the horizontal component of the photon $|\psi_r(t)\rangle = \frac{1}{\sqrt{2}}\left(e^{-2i\varphi_r(t)}|H\rangle + |V\rangle\right)$. The dynamics $|\psi_r(t)\rangle$ up to time t is obtained using the computer-controlled SLM: each spectral component of the photon passes through a different pixel and acquire a different phase $\varphi(t)$ determined by the computer according to the realizations of the simulated stochastic process. The second step consists in performing the ensemble average by recollecting the different components with a multimode optical fiber, as schematically shown in Fig. 4.1.

We remark here that the qubit system is described by the polarization degree of freedom of the photon, while the spectral degrees of freedom are effectively treated as the environment and will be traced out. Each spectral component is associated to a spatial direction $|x\rangle = |\omega(x)\rangle$ and if we introduce the notation $|\eta_r\rangle$ to describe the rth pixel satisfying the completeness relation, we have $|x\rangle = \sum_r \eta_r(x)|\eta_r\rangle$, where $\eta_r(x) = \langle\eta_r|x\rangle$, that is the projection of the component x on the rth pixel. We assume that the global system is initially in a factorized state and that the polarization is initialized in the state $|D\rangle = \frac{1}{\sqrt{2}}(|H\rangle + |V\rangle)$:

$$\rho_{SE}(0) = \rho_S(0) \otimes \rho_E = |D\rangle\langle D| \otimes \int d\omega |f(\omega)|^2 |\omega\rangle\langle\omega|, \tag{4.9}$$

which can be rewritten in terms of the pixel states as:

$$\rho_{SE}(0) = |D\rangle\langle D| \otimes \int dx |f(x)|^2 |x\rangle\langle x| = |D\rangle\langle D| \otimes \sum_{rs} A_{rs} |\eta_r\rangle\langle\eta_s|, \tag{4.10}$$

where

$$A_{rs} = \int dx |f(x)|^2 \eta_r(x) \eta_s^*(x). \tag{4.11}$$

Since on the horizontal component is imposed a pixel-dependent phase $\varphi_r(t)$, we can write the effective global evolution operator as:

$$U(t) = \exp\left[-2i|H\rangle\langle H| \otimes \sum_r \varphi_r(t) |\eta_r\rangle\langle\eta_r|\right], \tag{4.12}$$

which can be rewritten as:

$$U(t) = |H\rangle\langle H| \otimes \sum_r e^{-2i\varphi_r(t)} |\eta_r\rangle\langle\eta_r| + |V\rangle\langle V| \otimes \sum_r |\eta_r\rangle\langle\eta_r|\,. \tag{4.13}$$

The global evolved state $\rho_{SE}(t) = U(t)\rho_{SE}(0)U^\dagger(t)$ can be written in a compact notation as:

$$\rho_{SE}(t) = \frac{1}{1} \sum_{r,s} A_{rs} \begin{pmatrix} e^{-2i(\varphi_r(t)-\varphi_s(t))} |\eta_r\rangle\langle\eta_s| & e^{-2i\varphi_r(t)} |\eta_r\rangle\langle\eta_s| \\ e^{2i\varphi_r(t)} |\eta_r\rangle\langle\eta_s| & |\eta_r\rangle\langle\eta_s| \end{pmatrix} \tag{4.14}$$

and therefore the marginals are:

$$\rho_S(t) = \frac{1}{2} \sum_r A_{rr} \begin{pmatrix} 1 & e^{-2i\varphi_r(t)} \\ e^{2i\varphi_r(t)} & 1 \end{pmatrix} \tag{4.15}$$

$$\rho_E(t) = \sum_{r,s} A_{rs} \frac{1}{2} (e^{-2i(\varphi_r(t)-\varphi_s(t))} + 1) |\eta_r\rangle\langle\eta_s|. \tag{4.16}$$

Both the system and the environment are subject to a dephasing dynamics, where the populations do not evolve, while the off-diagonal elements are function of time. Let us focus on the expression of the system density matrix $\rho_S(t)$. Since the PDC spectrum $f(x)$ is almost constant in the considered range of values (cf. Fig. 4.2), the coefficients $A_{rr} = \int dx |f(x)|^2 |\eta_r(x)|^2 = n^{-1}$ become constant. Here n is the total number of pixels considered. It follows that the system density matrix becomes the one in (4.3), with

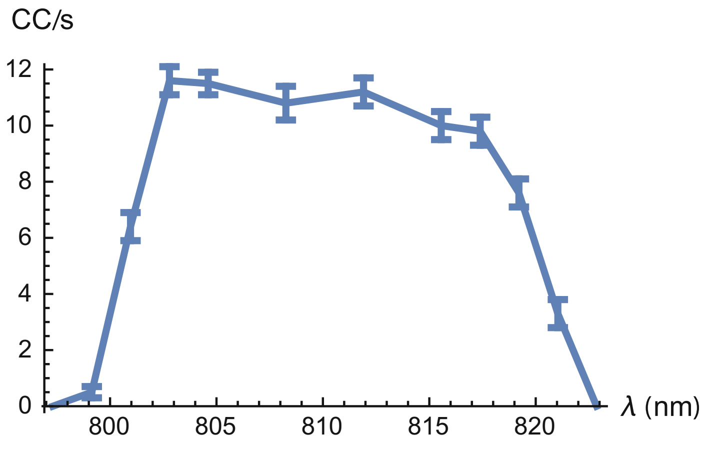

Fig. 4.2 The measured spectrum of the PDC. We can see that it is almost flat in the region 802–817 nm

$$\langle e^{2i\varphi(t)} \rangle_n = \frac{1}{n} \sum_{r=1}^{n} e^{2i\varphi_r(t)}. \tag{4.17}$$

This description is ideal and it does not consider the effects of imperfection and noise in the experimental apparatus. In order to give a more realistic representation of the system dynamics, we take into account the fact that the initial state of the system is not exactly pure, but a mixed state with high purity $\rho_{S,\exp}(t) = p\rho_S(t) + (1-p)\rho_{\text{mix}}$, where the parameter p is related to the purity of the initial state, with $p = 1$ corresponding to the pure state $\rho_S = |D\rangle\langle D|$ and $p = 0$ to the maximally mixed state $\rho_{\text{mix}} = \frac{1}{2}(|H\rangle\langle H| + |V\rangle\langle V|)$. The system density matrix (4.15) can now be rewritten as:

$$\rho_{S,\exp}(t) = \frac{1}{2} \begin{pmatrix} 1 & p\langle e^{-2i\varphi(t)} \rangle_n \\ p\langle e^{2i\varphi(t)} \rangle_n & 1 \end{pmatrix} \tag{4.18}$$

where the off-diagonal elements are now multiplied by the factor p. Equation (4.18) describes a dephasing map for a qubit. The off-diagonal elements of such evolutions, in addition to representing the coherences of the quantum state, are connected to the non-Makovianity of the dynamical map [5], which is nowadays considered a resource for quantum technologies [21]. For this reason we are interested in reconstructing the off-diagonal element of the density matrix and we assume that this value is a real quantity. Specifically, we want to reconstruct the maximized trace distance in (4.8). This can be experimentally done in two ways. The first approach consists in reconstructing the whole density matrix through qubit state tomography [19]. This means performing four projective measurements and to use their outputs to build a maximum likelihood estimator for the elements of the density matrix. The second approach exploits the fact that the off-diagonal coefficient is real to make only one projective measurement on the system. In particular, if we project onto the state $|D\rangle$, we obtain:

$$\langle D|\rho_{S,\exp}|D\rangle = \frac{1}{2}\left(1 + p\,\Re\langle e^{-2i\varphi(t)} \rangle_n\right) \tag{4.19}$$

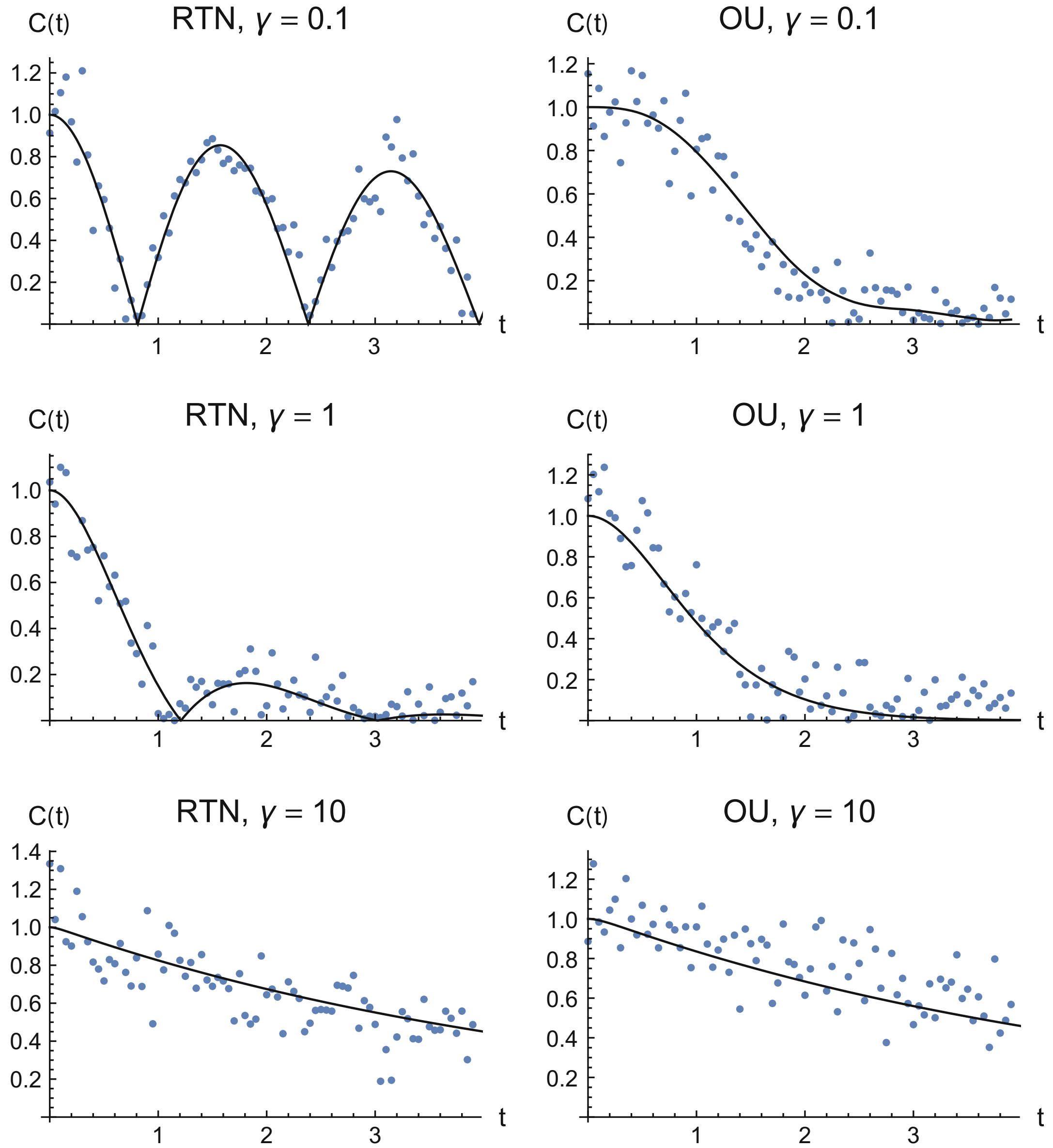

Fig. 4.3 Dynamics of the bsolute value of the off-diagonal element of $\rho_S(t)$, $C(t) = |\langle e^{-2i\varphi_r(t)}\rangle_n|$, for RTN (left) and OU (right), for $\gamma = 0.1$, $\gamma = 1$ and $\gamma = 10$ (from top to bottom). The blue dots are obtained experimentally by projection onto the state $|+\rangle$, corrected with the factor p, as discussed in the main text. The black line is the analytic solution of the model

which can easily give us the wanted quantity $C(t) = \left|\langle e^{-2i\varphi(t)}\rangle\right|$ my means of a single measurement. In order to obtain the experimental value of p we performed a reference measure in the presence of static noise (we considered the RTN with $\gamma = 0$) as described in [3].

It is worth noting that, because of the limited number of pixels of our SLM, the ensemble average is realized over a fixed number $n = 100$ of realizations of the fluctuating random fields. However, we show that this number is sufficient to correctly reproduce the theoretical behavior expected for NM, as can be seen in

Fig. 4.3, where we compare the simulated dynamics with the theoretical predictions. By changing the value of the switching rate γ, we are able to simulate the dynamics of the maximized trace distance $C(t)$ for the two different processes here considered. According to the theoretical model, we can move from a non-Markovian dynamics to a Markovian one for the RTN case by increasing the value of γ. Indeed, small values of γ lead to oscillations in the maximized trace distance, and the amplitude of these revivals is larger for smaller values of the switching rate. When the γ is above a certain threshold [5], the oscillations fade away and decoherence factor decays monotonically in time, meaning that memory effects do not play a role anymore in the dynamics. The OU process, instead, always leads to a monotonic behavior for $C(t)$, a signature of a Markovian quantum dynamics where information cannot flow back to the system.

4.4 Conclusions

We have suggested and demonstrated a quantum simulator based only on optical elements. This simulator can mimic the dynamics of single qubits in dephasing channels stemming from the interaction with classical fluctuating fields. The qubit is encoded in the polarization degrees of freedom of a single photon generated by PDC, while the several realizations of the classical noise are instead implemented on its spectral components by means of a programmable SLM. As proof of principle, we have shown that our simulator allows us to simulate quantum dynamics with different degrees of non-Markovianity, evaluated in terms of backflow of information from the environment to the system.

It is worth noting that our simulator can be also used to analyze the relation between the classical non-Markovianity of a classical fluctuating field and the non-Markovianity of the induced quantum dynamical map, by taking into account other kinds of stochastic processes. This will help to shed light into the open problem of finding a connection between the two definitions of non-Markovianity, used in the classical and quantum scenarios.

References

1. R.P. Feynman, Simulating physics with computers. Int. J. Theor. Phys. **21**, 467 (1982)
2. T.H. Johnson, S.R. Clark, D. Jaksch, What is a quantum simulator? EPJ Quant. Technol. **1**, 10 (2014)
3. S. Cialdi, M.A.C. Rossi, C. Benedetti, B. Vacchini, D. Tamascelli, S. Olivares, M.G.A. Paris, All-optical quantum simulator of qubit noisy channels. Appl. Phys. Lett. **110**, 081107 (2017)
4. M.A.C. Rossi, C. Benedetti, S. Cialdi, D. Tamascelli, S. Olivares, B. Vacchini, M.G.A. Paris, Non-Markovianity by undersampling in quantum optical simulators. Int. J. Quantum Inf. **15**, 1740009 (2017)
5. C. Benedetti, M.G.A. Paris, S. Maniscalco, Non-Markovianity of colored noisy channels. Phys. Rev. A **89**, 012114 (2014)

6. M.A.C. Rossi, C. Benedetti, M.G.A. Paris, Engineering decoherence for two-qubit systems interacting with a classical environment. Int. J. Quant. Inf. **12**, 1560003 (2014)
7. C. Benedetti, M.G.A. Paris, Effective dephasing for a qubit interacting with a transverse classical field. Int. J. Quant. Inf. **12**, 1461004 (2014)
8. M.A.C. Rossi, M.G.A. Paris, Non-Markovian dynamics of single- and two-qubit systems interacting with Gaussian and non-Gaussian fluctuating transverse environments. J. Chem. Phys. **144**, 024113 (2016)
9. H.J. Wold, H. Brox, Y.M. Galperin, J. Bergli, Decoherence of a qubit due to either a quantum fluctuator, or classical telegraph noise. Phys. Rev. B **86**, 205404 (2012)
10. A. Rivas, S.F. Huelga, M.B. Plenio, Entanglement and Non-Markovianity of quantum evolutions. Phys. Rev. Lett. **105**, 050403 (2010)
11. S. Lorenzo, F. Plastina, M. Paternostro, Geometrical characterization of non-Markovianity. Phys. Rev. A **88**, 020102(R) (2013)
12. X.-M. Lu, X. Wang, C.P. Sun, Quantum Fisher information flow and non-Markovian processes of open systems. Phys. Rev. A **82**, 042103 (2010)
13. H.-P. Breuer, E.M. Laine, J. Piilo, Measure for the degree of non-Markovian behavior of quantum processes in open systems. Phys. Rev. Lett. **103**, 210401 (2009)
14. Z. He, J. Zou, L. Li, B. Shao, Effective method of calculating the non-Markovianity N for single-channel open systems. Phys. Rev. A **83**, 012108 (2011)
15. A.W. Chin, S.F. Huelga, M.B. Plenio, Quantum metrology in non-Markovian environments. Phys. Rev. Lett. **109**, 233601 (2012)
16. R. Vasile, S. Olivares, M.G.A. Paris, S. Maniscalco, Continuous variable quantum key distribution in non-Markovian channels. Phys. Rev. A **83**, 042321 (2011)
17. S.F. Huelga, A. Rivas, M.B. Plenio, Non-Markovianity-assisted steady state entanglement. Phys. Rev. Lett. **108**, 160402 (2012)
18. A.M. Weiner, Femtosecond pulse shaping using spatial light modulators. Rev. of Sci. Instrum. **71**, 1929 (2000)
19. D.F.V. James, P.G. Kwiat, W.J. Munro, A.G. White, Measurement of qubits. Phys. Rev. A **64**, 052312 (2001)
20. K. Banaszek, G.M. D'Ariano, M.G.A. Paris, M.F. Sacchi, Maximum-likelihood estimation of the density matrix. Phys. Rev. A **61**, 010304(R) (1999)
21. B. Bylicka, D. Chruściński, S. Maniscalco, Non-Markovianity and reservoir memory of quantum channels: a quantum information theory perspective. Sci. Rep. **4**, 5720 (2014)